

## 218318: muscovite–chlorite schist, Palms Yard

(Winnama Formation, Central Zone, Lamboo Province)

### Location and sampling

DIXON RANGE (SE 52-6), TURKEY CREEK (4563)  
MGA Zone 52, 420687E 8094688N

Sampled on 2 June 2015

This sample was collected from a low outcrop on the eastern bank of Turkey Creek on Osmond Valley Station, about 8.1 km southwest of Mount Parker, 5.0 km south of Winnama Yard, and 1.0 km north-northwest of Palms Yard.

### Tectonic unit/relations

The unit sampled is a metasedimentary schist assigned to the 1845–1840 Ma Winnama Formation of the Central Zone of the Lamboo Province (Tyler et al., 1997). The Winnama Formation consists of metamorphosed greywacke, lithic sandstone, siltstone, mudstone, basalt, dolerite, and carbonate rocks including calcareous siltstone and sandstone (Tyler et al., 1997). At this locality, the schist is intruded by granitic dykes 15–20 cm thick that post-date an early layer-parallel foliation and are interpreted to have been deformed by two generations of folding (Fig. 1).

### Petrographic description

The sample is a fine-grained, strongly foliated muscovite–chlorite schist, consisting of about 65% quartz, 15–18% feldspar, 12% muscovite, 5% chlorite, and accessory tourmaline, hematite and zircon. Quartz occurs as anhedral, equant to elongate grains up to 1 mm in size, although the average grain size is 0.3 – 0.4 mm; some grains are strained and/or subgrained but not finely recrystallized. Feldspar also occurs as anhedral grains with a similar size range to quartz and these two minerals form a granoblastic texture. The majority of feldspar grains are at least lightly sericitized. Some grains show multiple twinning indicating plagioclase, and the amount of K-feldspar, if any, is unclear. Muscovite and chlorite, the latter possibly retrogressed biotite, occur as strongly aligned anhedral and subhedral laths up to 0.5 mm long. Muscovite forms continuous folia, which are slightly deflected around the margins of the larger quartz and feldspar grains, without development of pressure shadows. Although micas define a strong schistosity in the sample, many quartz and feldspar grains are also aligned parallel to it. Granoblastic textures in the quartz–feldspar aggregate and the relatively low strain observed in these minerals may indicate syn- to late-tectonic crystallization. The metamorphic grade is at least greenschist facies.

### Zircon morphology

Zircons isolated from this sample are colourless to dark brown and opaque, anhedral to subhedral, and variably rounded. The crystals are up to 350  $\mu\text{m}$  long, and equant to elongate, with aspect ratios up to 6:1. In cathodoluminescence (CL) images, concentric zoning is ubiquitous. Many crystals are dominated by high-uranium, metamict domains. Some crystals have pitted outer surfaces and concentric zoning truncated at grain boundaries, features consistent with sedimentary transport. A CL image of representative zircons is shown in Figure 2.

### Analytical details

This sample was analysed over three sessions on 19–21 and 23–24 January 2017, using SHRIMP-A. Analyses 1.1 to 27.1 (spot numbers 1–27) were obtained during the first session, together with 21 analyses of the M257 standard. Significant drift of standard  $^{238}\text{U}/^{206}\text{Pb}^*$  dates during the first session was addressed by fitting a LOWESS curve (Cleveland, 1979) with a smoothing window of 21 analyses, implemented using the program Isoplot 2.50 (Ludwig, 2009; Wingate and Lu, 2018). During this session, 21 standard analyses indicated an external spot-to-spot (reproducibility) uncertainty of 0.50% ( $1\sigma$ ). Isotopic mass fractionation of  $^{207}\text{Pb}/^{206}\text{Pb}$  ratios during the first session was corrected by reference to the OGC1 standard; measured ratios were increased by 0.94%. Analyses 28.1 to 56.1 (spot numbers 28–56) were obtained during the second session, together with seven analyses of the M257 standard, which indicated an external spot-to-spot (reproducibility) uncertainty of 0.50% ( $1\sigma$ ) and a  $^{238}\text{U}/^{206}\text{Pb}^*$  calibration uncertainty of 0.33% ( $1\sigma$ ). Isotopic mass fractionation of  $^{207}\text{Pb}/^{206}\text{Pb}$  ratios during the second session was corrected by reference to the OGC1 standard; measured ratios were increased by 0.80%. Analyses 57.1 to 80.1 (spot numbers 57–81) were obtained during the third session, together with six analyses of the M257 standard, of which five analyses indicated an external spot-to-spot (reproducibility) uncertainty of 0.50% ( $1\sigma$ ) and a  $^{238}\text{U}/^{206}\text{Pb}^*$  calibration uncertainty of 0.29% ( $1\sigma$ ). Isotopic mass fractionation of  $^{207}\text{Pb}/^{206}\text{Pb}$  ratios during the third session was corrected by reference to the OGC1 standard; measured ratios were increased by 0.55%. Calibration uncertainties are included in the errors of  $^{238}\text{U}/^{206}\text{Pb}^*$  ratios and dates listed in Table 1. Common-Pb corrections were applied to all analyses using contemporaneous isotopic compositions determined according to the model of Stacey and Kramers (1975).



**Figure 1.** Outcrop image for sample 218318: muscovite–chlorite schist, Palms Yard

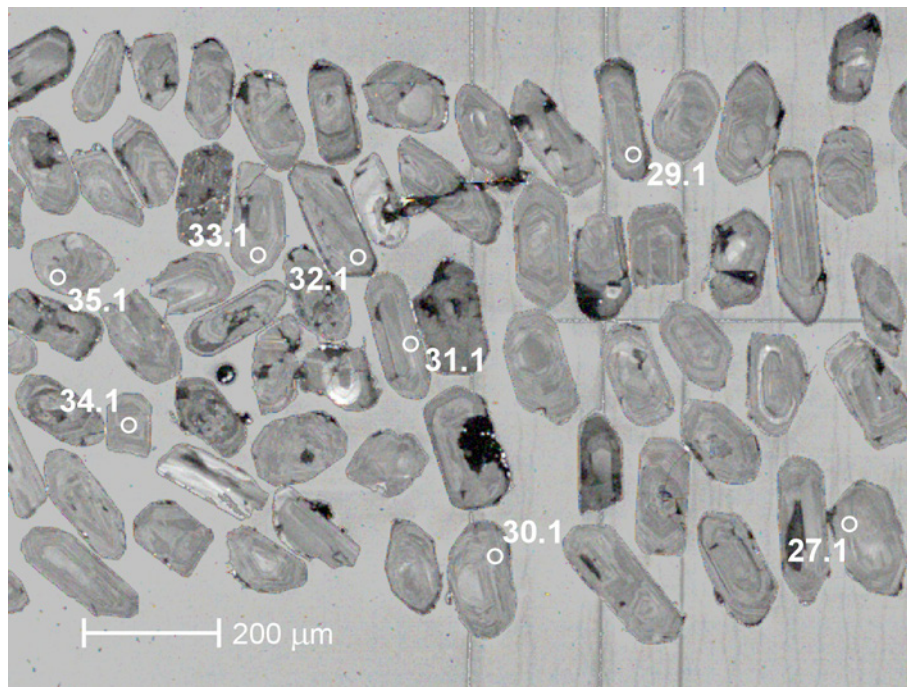


**Figure 2.** Cathodoluminescence image of representative zircons from sample 218318: muscovite–chlorite schist, Palms Yard. Numbered circles indicate the approximate locations of analysis sites

Table 1. Ion microprobe analytical results for zircons from sample 218318: muscovite–chlorite schist, Palms Yard

Group ID	Spot no.	Grain. spot	$^{238}\text{U}$ (ppm)	$^{232}\text{Th}$ (ppm)	$\frac{^{232}\text{Th}}{^{238}\text{U}}$	$f_{204}$ (%)	$^{238}\text{U}/^{206}\text{Pb} \pm 1\sigma$	$^{207}\text{Pb}/^{206}\text{Pb} \pm 1\sigma$	$^{238}\text{U}/^{206}\text{Pb}^* \pm 1\sigma$	$^{207}\text{Pb}^*/^{206}\text{Pb}^* \pm 1\sigma$	$^{238}\text{U}/^{206}\text{Pb}^*$ date (Ma) $\pm 1\sigma$	$^{207}\text{Pb}^*/^{206}\text{Pb}^*$ date (Ma) $\pm 1\sigma$	Disc. (%)						
Y	36	36.1	321	120	0.37	0.063	3.113	0.038	0.11336	0.00075	3.115	0.038	0.11280	0.00078	1795	19	1845	12	2.7
S	48	48.1	265	75	0.28	-0.030	3.057	0.037	0.11256	0.00080	3.056	0.037	0.11282	0.00081	1825	20	1845	13	1.1
S	73	72.1	281	63	0.22	0.133	3.103	0.036	0.11406	0.00106	3.107	0.036	0.11288	0.00117	1799	18	1846	19	2.6
S	72	2.2	318	93	0.29	0.138	3.062	0.034	0.11410	0.00103	3.066	0.034	0.11289	0.00113	1820	18	1846	18	1.4
S	34	34.1	256	123	0.48	0.079	3.116	0.027	0.11419	0.00080	3.119	0.027	0.11349	0.00083	1793	14	1856	13	3.4
S	33	33.1	228	86	0.38	0.042	3.006	0.042	0.11388	0.00081	3.008	0.042	0.11352	0.00083	1851	23	1857	13	0.3
S	1	1.1	304	162	0.53	0.053	3.008	0.025	0.11408	0.00081	3.010	0.025	0.11362	0.00083	1849	13	1858	13	0.5
S	65	65.1	394	152	0.39	0.061	3.138	0.033	0.11419	0.00095	3.140	0.033	0.11365	0.00099	1782	16	1859	16	4.1
S	40	40.1	238	94	0.39	0.011	3.003	0.027	0.11387	0.00082	3.003	0.027	0.11377	0.00083	1853	15	1861	13	0.4
S	28	28.1	354	307	0.87	0.000	3.047	0.025	0.11382	0.00073	3.047	0.025	0.11382	0.00073	1830	13	1861	12	1.7
S	16	16.1	442	134	0.30	0.021	3.020	0.023	0.11417	0.00073	3.021	0.023	0.11399	0.00074	1843	12	1864	12	1.1
S	13	13.1	319	85	0.27	0.065	3.015	0.027	0.11470	0.00079	3.017	0.027	0.11413	0.00081	1846	14	1866	13	1.1
S	55	55.1	379	272	0.72	-0.021	3.108	0.025	0.11419	0.00073	3.108	0.025	0.11437	0.00074	1798	13	1870	12	3.8
S	9	9.1	110	45	0.42	0.000	3.037	0.036	0.11452	0.00217	3.037	0.036	0.11452	0.00217	1835	19	1872	34	2.0
S	26	26.1	423	143	0.34	0.046	2.953	0.022	0.11497	0.00072	2.955	0.022	0.11457	0.00074	1879	12	1873	12	-0.3
S	39	39.1	301	45	0.15	0.043	3.021	0.026	0.11500	0.00077	3.022	0.026	0.11462	0.00079	1843	14	1874	12	1.7
S	66	66.1	248	47	0.19	0.000	3.077	0.036	0.11469	0.00110	3.077	0.036	0.11469	0.00110	1814	19	1875	17	3.2
S	41	41.1	378	88	0.23	0.000	3.005	0.024	0.11502	0.00072	3.005	0.024	0.11502	0.00072	1852	13	1880	11	1.5
S	45	45.1	266	41	0.15	0.105	3.075	0.027	0.11610	0.00079	3.078	0.027	0.11517	0.00084	1814	14	1883	13	3.7
S	6	6.1	467	80	0.17	0.188	3.113	0.023	0.11683	0.00071	3.119	0.023	0.11518	0.00079	1793	12	1883	12	4.8
S	61	61.1	399	66	0.17	-0.043	3.102	0.032	0.11485	0.00093	3.100	0.032	0.11523	0.00096	1802	16	1884	15	4.3
S	14	14.1	212	118	0.56	0.014	3.015	0.028	0.11536	0.00088	3.015	0.028	0.11523	0.00089	1846	15	1884	14	2.0
S	42	42.1	523	59	0.11	0.009	3.050	0.023	0.11549	0.00068	3.051	0.023	0.11542	0.00068	1828	13	1886	11	3.1
S	80	79.1	179	41	0.23	0.032	3.008	0.040	0.11583	0.00124	3.009	0.040	0.11554	0.00127	1850	21	1888	20	2.0
S	57	57.1	543	32	0.06	0.042	3.102	0.030	0.11605	0.00091	3.103	0.030	0.11567	0.00093	1801	15	1890	14	4.7
S	38	38.1	131	49	0.37	-0.042	2.986	0.032	0.11613	0.00102	2.985	0.032	0.11649	0.00105	1863	18	1903	16	2.1
S	69	69.1	182	84	0.46	0.154	2.634	0.036	0.13729	0.00134	2.638	0.036	0.13592	0.00147	2072	24	2176	19	4.8
S	46	46.1	157	74	0.47	0.011	2.341	0.023	0.15135	0.00094	2.342	0.023	0.15125	0.00095	2292	20	2360	11	2.9
S	24	24.1	209	49	0.23	0.061	2.271	0.021	0.15257	0.00092	2.272	0.021	0.15202	0.00095	2351	18	2369	11	0.7
S	76	75.1	132	130	0.98	0.163	2.201	0.033	0.16290	0.00142	2.205	0.033	0.16144	0.00154	2411	30	2471	16	2.4

Table 1. continued

Group ID	Spot no.	Grain. spot	<sup>238</sup> U (ppm)	<sup>232</sup> Th (ppm)	<sup>232</sup> Th/ <sup>238</sup> U	f <sub>204</sub> (%)	<sup>238</sup> U/ <sup>206</sup> Pb ± 1σ	<sup>207</sup> Pb/ <sup>206</sup> Pb ± 1σ	<sup>238</sup> U/ <sup>206</sup> Pb* ± 1σ	<sup>207</sup> Pb*/ <sup>206</sup> Pb* ± 1σ	<sup>238</sup> U/ <sup>206</sup> Pb* date (Ma) ± 1σ	<sup>207</sup> Pb*/ <sup>206</sup> Pb* date (Ma) ± 1σ	Disc. (%)						
P	2	2.1	395	136	0.34	0.031	3.007	0.023	0.11041	0.00125	3.008	0.023	0.11014	0.00126	1850	12	1802	21	-2.7
D	64	64.1	1023	6	0.01	0.178	7.535	0.063	0.08349	0.00083	7.548	0.064	0.08198	0.00094	802	6	1245	22	35.6
D	44	44.1	845	231	0.27	0.173	8.317	0.085	0.08591	0.00069	8.331	0.085	0.08442	0.00076	731	7	1302	17	43.9
D	74	73.1	919	327	0.36	0.212	7.180	0.085	0.08894	0.00086	7.196	0.086	0.08712	0.00098	839	9	1363	22	38.5
D	49	49.1	942	288	0.31	0.066	6.408	0.046	0.09218	0.00066	6.412	0.046	0.09161	0.00068	934	6	1459	14	36.0
D	15	15.1	706	224	0.32	0.142	6.316	0.043	0.09529	0.00073	6.325	0.043	0.09407	0.00079	946	6	1509	16	37.3
D	53	53.1	813	89	0.11	0.132	5.948	0.043	0.09676	0.00068	5.956	0.043	0.09562	0.00073	1001	7	1540	14	35.0
D	23	23.1	622	137	0.22	0.122	5.588	0.039	0.09916	0.00072	5.595	0.039	0.09809	0.00077	1060	7	1588	15	33.3
D	75	74.1	745	233	0.31	0.471	5.310	0.076	0.10370	0.00089	5.335	0.076	0.09961	0.00118	1108	15	1617	22	31.5
D	31	31.1	630	79	0.13	0.154	5.111	0.040	0.10264	0.00128	5.119	0.040	0.10130	0.00131	1150	8	1648	24	30.2
D	71	71.1	567	318	0.56	0.203	5.109	0.048	0.10341	0.00099	5.119	0.048	0.10164	0.00111	1150	10	1654	20	30.5
D	70	70.1	698	62	0.09	0.199	5.035	0.045	0.10396	0.00088	5.045	0.045	0.10223	0.00098	1166	10	1665	18	30.0
D	7	7.1	652	106	0.16	0.051	4.136	0.029	0.10332	0.00069	4.138	0.029	0.10288	0.00071	1395	9	1677	13	16.8
D	20	20.1	589	140	0.24	0.102	4.633	0.035	0.10542	0.00073	4.637	0.035	0.10452	0.00077	1259	9	1706	14	26.2
D	22	22.1	593	165	0.28	0.106	4.526	0.034	0.10663	0.00073	4.531	0.034	0.10570	0.00077	1286	9	1727	13	25.5
D	4	4.1	495	67	0.13	0.101	4.457	0.032	0.10665	0.00075	4.461	0.032	0.10577	0.00079	1304	9	1728	14	24.5
D	29	29.1	672	95	0.14	0.100	4.290	0.031	0.10684	0.00066	4.295	0.031	0.10597	0.00069	1349	9	1731	12	22.1
D	21	21.1	548	47	0.09	0.162	4.495	0.085	0.10770	0.00073	4.502	0.085	0.10628	0.00079	1293	22	1737	14	25.5
D	77	76.1	610	221	0.36	0.198	4.045	0.037	0.10861	0.00088	4.053	0.037	0.10687	0.00098	1422	12	1747	17	18.6
D	81	80.1	554	261	0.47	0.188	4.062	0.038	0.10885	0.00091	4.070	0.039	0.10720	0.00102	1416	12	1752	17	19.2
D	60	60.1	515	90	0.17	0.091	3.924	0.038	0.10824	0.00092	3.928	0.038	0.10745	0.00098	1462	13	1757	17	16.8
D	56	56.1	637	290	0.45	0.123	4.168	0.033	0.10856	0.00068	4.173	0.033	0.10748	0.00072	1385	10	1757	12	21.2
D	8	8.1	398	115	0.29	0.000	4.249	0.045	0.10766	0.00077	4.249	0.045	0.10766	0.00077	1363	13	1760	13	22.6
D	63	63.1	573	66	0.11	0.144	4.279	0.041	0.10923	0.00092	4.285	0.041	0.10796	0.00100	1352	12	1765	17	23.4
D	68	68.1	489	135	0.28	0.192	3.384	0.033	0.11117	0.00177	3.390	0.033	0.10948	0.00182	1666	15	1791	30	6.9
D	10	10.1	579	199	0.34	0.099	3.605	0.039	0.11100	0.00070	3.609	0.039	0.11012	0.00073	1577	15	1801	12	12.5
D	43	43.1	489	165	0.34	0.107	3.682	0.029	0.11211	0.00071	3.686	0.029	0.11116	0.00075	1547	11	1818	12	14.9
D	78	77.1	578	47	0.08	0.042	3.474	0.032	0.11185	0.00085	3.475	0.032	0.11148	0.00087	1630	13	1824	14	10.6



Table 1. continued

Group ID	Spot no.	Grain. spot	$^{238}\text{U}$ (ppm)	$^{232}\text{Th}$ (ppm)	$\frac{^{232}\text{Th}}{^{238}\text{U}}$	$f_{204}$ (%)	$^{238}\text{U}/^{206}\text{Pb} \pm 1\sigma$	$^{207}\text{Pb}/^{206}\text{Pb} \pm 1\sigma$	$^{238}\text{U}/^{206}\text{Pb}^* \pm 1\sigma$	$^{207}\text{Pb}^*/^{206}\text{Pb}^* \pm 1\sigma$	$^{238}\text{U}/^{206}\text{Pb}^*$ date (Ma) $\pm 1\sigma$	$^{207}\text{Pb}^*/^{206}\text{Pb}^*$ date (Ma) $\pm 1\sigma$	Disc. (%)						
D	30	30.1	594	201	0.34	0.067	3.529	0.026	0.11249	0.00067	3.532	0.026	0.11191	0.00069	1607	11	1831	11	12.2
D	51	51.1	347	89	0.26	0.008	3.302	0.027	0.11212	0.00074	3.302	0.027	0.11205	0.00075	1705	13	1833	12	7.0
D	62	62.1	306	110	0.36	0.246	4.130	0.047	0.11439	0.00120	4.140	0.047	0.11223	0.00142	1395	14	1836	23	24.0
D	47	47.1	395	129	0.33	0.087	4.246	0.047	0.11310	0.00077	4.249	0.047	0.11233	0.00081	1362	14	1837	13	25.9
D	25	25.1	443	164	0.37	0.050	3.290	0.037	0.11286	0.00073	3.292	0.037	0.11243	0.00075	1710	17	1839	12	7.0
D	12	12.1	462	230	0.50	0.042	3.905	0.066	0.11283	0.00135	3.906	0.066	0.11246	0.00136	1469	22	1839	22	20.1
D	58	58.1	224	62	0.28	0.086	3.507	0.043	0.11324	0.00116	3.510	0.043	0.11249	0.00124	1616	18	1840	20	12.2
D	32	32.1	330	85	0.26	0.000	3.246	0.027	0.11271	0.00075	3.246	0.027	0.11271	0.00075	1731	13	1844	12	6.1
D	5	5.1	219	123	0.56	0.155	4.162	0.067	0.11423	0.00091	4.168	0.067	0.11286	0.00101	1386	20	1846	16	24.9
D	54	54.1	324	54	0.17	0.025	3.241	0.027	0.11325	0.00076	3.242	0.027	0.11303	0.00077	1733	13	1849	12	6.2
D	3	3.1	451	115	0.25	0.052	3.302	0.025	0.11380	0.00074	3.304	0.025	0.11334	0.00076	1704	11	1854	12	8.0
D	67	67.1	330	134	0.41	0.074	3.620	0.039	0.11406	0.00101	3.623	0.039	0.11340	0.00106	1571	15	1855	17	15.3
D	50	50.1	264	100	0.38	0.051	3.276	0.029	0.11407	0.00081	3.278	0.029	0.11363	0.00083	1717	13	1858	13	7.6
D	59	59.1	287	126	0.44	0.040	3.176	0.036	0.11466	0.00103	3.178	0.036	0.11431	0.00106	1764	18	1869	17	5.6
D	37	37.1	522	164	0.31	-0.005	3.316	0.033	0.11433	0.00069	3.316	0.033	0.11437	0.00069	1699	15	1870	11	9.1
D	52	52.1	326	86	0.26	0.111	3.327	0.028	0.11556	0.00081	3.330	0.028	0.11458	0.00085	1693	13	1873	13	9.6
D	79	78.1	396	69	0.17	0.079	3.206	0.033	0.11540	0.00096	3.208	0.033	0.11471	0.00101	1749	16	1875	16	6.7
D	27	27.1	311	73	0.23	0.047	3.408	0.028	0.11530	0.00084	3.409	0.028	0.11488	0.00086	1658	12	1878	14	11.7
D	19	19.1	111	53	0.48	-0.169	3.306	0.039	0.11417	0.00121	3.300	0.039	0.11566	0.00137	1706	18	1890	21	9.7
D	11	11.1	365	168	0.46	0.008	2.909	0.025	0.12606	0.00078	2.909	0.025	0.12599	0.00078	1905	14	2043	11	6.8
D	18	18.1	239	108	0.45	0.012	3.427	0.031	0.12949	0.00147	3.428	0.031	0.12939	0.00147	1650	13	2090	20	21.0
D	17	17.1	370	287	0.77	0.031	3.067	0.024	0.15463	0.00085	3.068	0.024	0.15435	0.00086	1819	13	2395	10	24.1
D	35	35.1	350	224	0.64	0.035	2.843	0.023	0.15888	0.00081	2.844	0.023	0.15857	0.00082	1942	14	2440	9	20.4

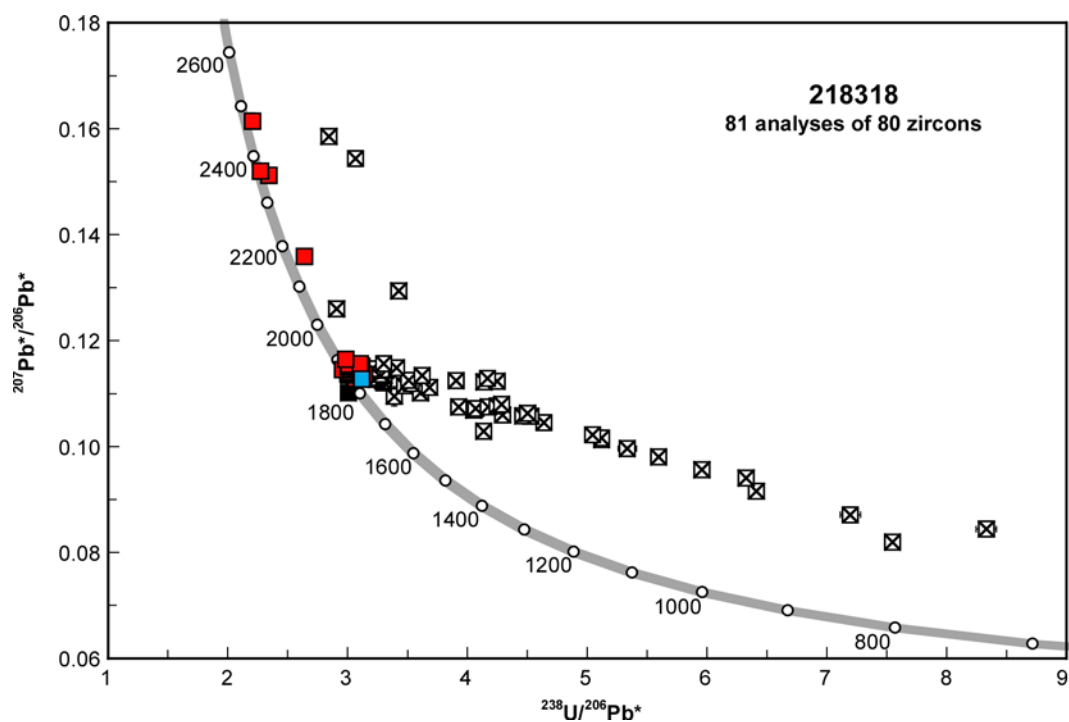


Figure 3. U–Pb analytical data for zircons from sample 218318: muscovite–chlorite schist, Palms Yard. Blue square indicates Group Y (youngest detrital zircon); red squares indicate Group S (older detrital zircons); Black square indicates Group P (radiogenic lead loss); crossed squares indicate Group D (discordance >5%)

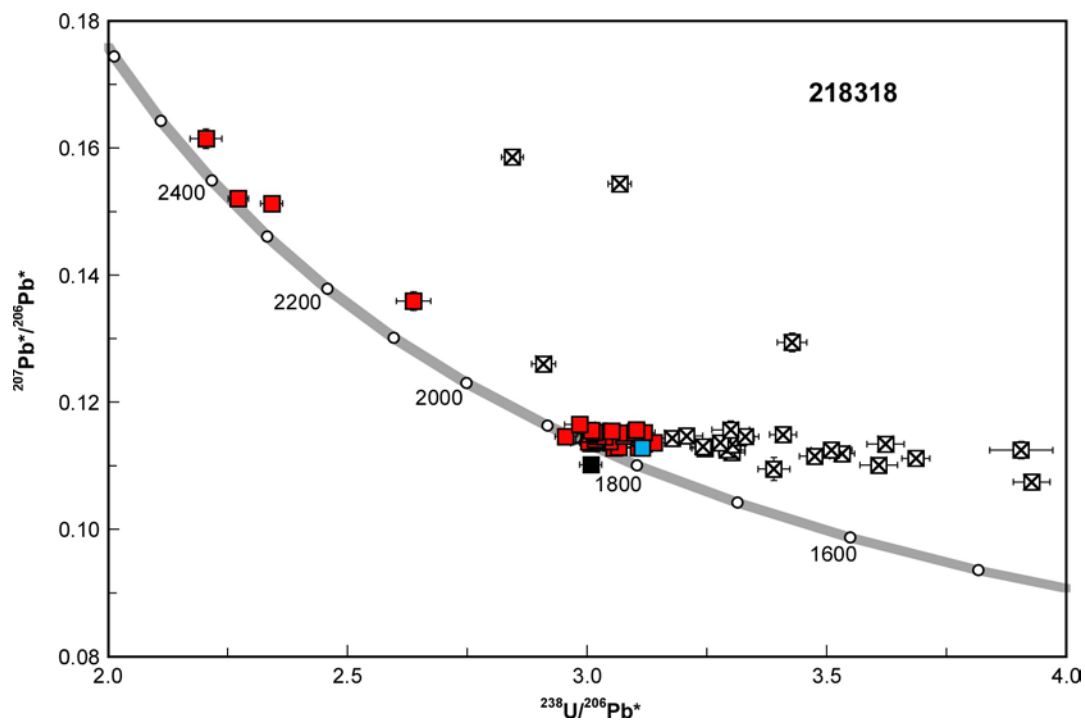


Figure 4. Expanded view of U–Pb analytical data for zircons from sample 218318: muscovite–chlorite schist, Palms Yard. Symbols as in Figure 3)

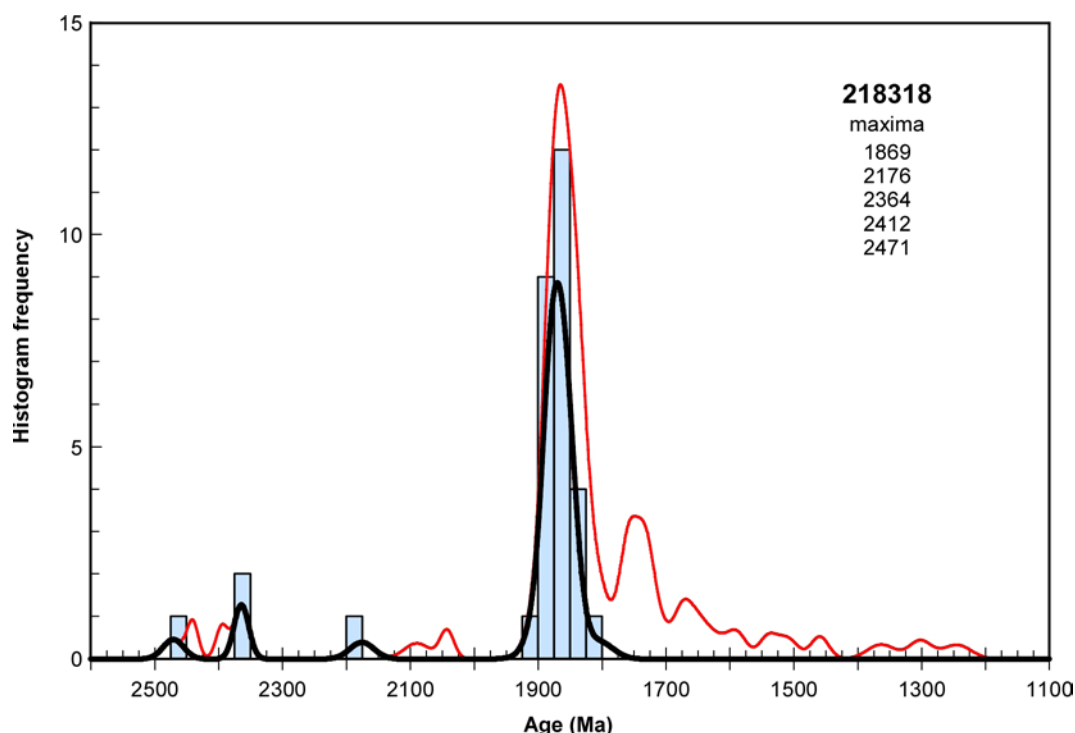


Figure 5. Expanded view of U–Pb analytical data for zircons from sample 218318: muscovite–chlorite schist, Palms Yard. Symbols as in Figure 3

## Results

Eighty-one analyses were obtained from 80 zircons. Results are listed in Table 1, and shown in concordia diagrams (Figs 3, 4), and a probability density diagram (Fig. 5).

## Interpretation

The analyses are concordant to strongly discordant (Figs 3, 4). Fifty analyses are >5% discordant. The dates obtained from these 50 analyses (Group D; Table 1) are unreliable, and are considered not to be geologically significant. The remaining 31 analyses can be divided into three groups, based on their  $^{207}\text{Pb}^*/^{206}\text{Pb}^*$  ratios.

Group Y comprises one analysis (Table 1), which yields a  $^{207}\text{Pb}^*/^{206}\text{Pb}^*$  date of  $1845 \pm 12$  Ma ( $1\sigma$ ).

Group S comprises 29 analyses of 29 zircons (Table 1), which yield  $^{207}\text{Pb}^*/^{206}\text{Pb}^*$  dates of 2471–1845 Ma.

Group P comprises one analysis (Table 1), which yields a  $^{207}\text{Pb}^*/^{206}\text{Pb}^*$  date of  $1802 \pm 21$  Ma ( $1\sigma$ ).

It is possible that all of the analyses in Group Y and S are of unmodified detrital zircons, in which case the date of  $1845 \pm 12$  Ma ( $1\sigma$ ) for the single analysis in Group Y represents a maximum age of deposition for the sedimentary protolith. A more conservative estimate of the maximum depositional age can be based on the weighted mean  $^{207}\text{Pb}^*/^{206}\text{Pb}^*$  date of  $1870 \pm 6$  Ma (MSWD = 1.2) for the 26 youngest analyses in Groups Y and S.

The data for combined Groups Y and S indicate a significant age component at c. 1869 Ma (Fig. 5), based on contributions from approximately 25 analyses. This is interpreted as the age of the dominant zircon-crystallizing

rock in the detrital source region, or the age of a detrital component within sediments that have been reworked into this rock.

The date of  $1802 \pm 21$  Ma ( $1\sigma$ ) for the single analysis in Group P is significantly younger than a second analysis on the same grain, and therefore interpreted to reflect ancient loss of radiogenic lead.

## References

- Cleveland, WS 1979, Robust, locally weighted regression and smoothing scatterplots: *Journal of the American Statistical Association*, v. 74, p. 829–836.
- Ludwig, KR 2009, *Squid 2.50, A User's Manual*: Berkeley Geochronology Centre, Berkeley, California, USA, 95p. (unpublished report).
- Stacey, JS and Kramers, JD 1975, Approximation of terrestrial lead isotope evolution by a two-stage model: *Earth and Planetary Science Letters*, v. 26, p. 207–221.
- Tyler, IM, Thorne, AM, Hoatson, DM and Blake, DH 1997, Turkey Creek, 1:100 000 geological sheet 4563, Geological Survey of Western Australia.
- Wingate, MTD and Lu, Y 2018, *Introduction to geochronology information 2018*: Geological Survey of Western Australia, 5p.

## Recommended reference for this publication

- Lu, Y, Wingate, MTD, Maidment, DW and Phillips, C 2018, 218318: muscovite–chlorite schist, Palms Yard; *Geochronology Record* 1544: Geological Survey of Western Australia, 7p.

Data obtained: 24 January 2017

Data released: 12 December 2018